

Sulforaphane effects on postinfarction cardiac remodeling in rats: modulation of redox-sensitive prosurvival and proapoptotic proteins

Rafael Oliveira Fernandes^a, Alexandre Luz De Castro^{a,b}, Jéssica Hellen Poletto Bonetto^a,
Vanessa Duarte Ortiz^a, Dalvana Daneliza Müller^a, Cristina Campos-Carraro^a, Silvia Barbosa^c,
Laura Tartari Neves^d, Léder Leal Xavier^d, Paulo Cavalheiro Schenkel^a, Pawan Singal^e, Neelam Khaper^f,
Alex Sander da Rosa Araujo^a, Adriane Belló-Klein^{a,*}

^aLaboratory of Cardiovascular Physiology, Institute of Basic Health Science, Federal University of Rio Grande do Sul, Porto Alegre, Rio Grande do Sul, Brazil

^bCentro Universitário Ritter dos Reis (Uniritter), Porto Alegre, Rio Grande do Sul, Brazil

^cLaboratório de Histofisiologia Comparada, Departamento de Ciências Morfológicas, Instituto de Ciências Básicas da Saúde, Federal University of Rio Grande do Sul, Porto Alegre, Rio Grande do Sul, Brazil

^dLaboratório de Biologia Celular e Tecidual, Departamento de Ciências Morfofisiológicas, Faculdade de Biociências, Pontifícia Universidade Católica do Rio Grande do Sul, Porto Alegre, Rio Grande do Sul, Brazil

^eInstitute of Cardiovascular Sciences, St. Boniface General Hospital Research Centre, Winnipeg, Manitoba, Canada

^fMedical Sciences Division, Northern Ontario School of Medicine, Lakehead University, Thunder Bay, Ontario, Canada

Received 7 March 2016; received in revised form 26 April 2016; accepted 11 May 2016

Abstract

This study investigated whether sulforaphane (SFN), a compound found in cruciferous vegetables, could attenuate the progression of post-myocardial infarction (MI) cardiac remodeling. Male Wistar rats (350 g) were allocated to four groups: SHAM ($n = 8$), SHAM + SFN ($n = 7$), MI ($n = 8$) and MI + SFN ($n = 5$). On the third day after surgery, cardiac function was assessed and SFN treatment (5 mg/kg/day) was started. At the end of 25 days of treatment, cardiac function was assessed and heart was collected to measure collagen content, oxidative stress and protein kinase. MI and MI + SFN groups presented cardiac dysfunction, without signs of congestion. Sulforaphane reduced fibrosis (2.1-fold) in infarcted rats, which was associated with a slight attenuation in the cardiac remodeling process. Both infarcted groups presented increases in the oxidative markers xanthine oxidase and 4-hydroxynonenal, as well as a parallel increase in the antioxidant enzymes glutathione peroxidase and superoxide dismutase. Moreover, sulforaphane stimulated the cytoprotective heme oxygenase-1 (HO-1) (38%). Oxidative markers correlated with ERK 1/2 activation. In the MI + SFN group, up-regulation of ERK 1/2 (34%) and Akt (35%), as well as down-regulation of p38 (52%), was observed. This change in the prosurvival kinase balance in the MI + SFN group was related to a down-regulation of apoptosis pathways (Bax/Bcl-2/caspase-3). Sulforaphane was unable to modulate autophagy. Taken together, sulforaphane increased HO-1, which may generate a redox environment in the cardiac tissue favorable to activation of prosurvival and deactivation of prodeath pathways. In conclusion, this natural compound contributes to attenuation of the fibrotic process, which may contribute to mitigation against the progression of cardiac remodeling postinfarction.

© 2016 Elsevier Inc. All rights reserved.

Keywords: Myocardial infarction; Heart failure; Isothiocyanate; Heme oxygenase-1; Oxidative stress; Autophagy

1. Introduction

Postinfarction cardiac pathological remodeling is characterized by ventricular chamber dilation, cardiac hypertrophy and fibrosis due to cardiomyocyte death, inflammation, myocyte growth and fibroblast proliferation [1,2]. Interventions to decrease or delay this set of

mechanisms are fundamental to preventing the progression of cardiac dysfunction and, ultimately, heart failure.

A common event in the pathogenesis of cardiac remodeling is oxidative stress, which contributes to cardiac dysfunction [3–6]. Excessive levels of reactive oxygen species (ROS) that result in oxidative stress have been associated with apoptosis, necrosis and autophagy [7–9]. Apoptosis has been identified as an essential process in cardiac remodeling and progression to heart failure [10,11]. Autophagy is an important process protecting cardiomyocytes from ischemic injury whereas impaired autophagy is known to contribute to adverse cardiac remodeling [12,13]. Maladaptive autophagy has also been reported to contribute to the progression from cardiac hypertrophy to decompensated heart failure [14]. These studies

* Corresponding author. Laboratório de Fisiologia Cardiovascular, Departamento de Fisiologia, Universidade Federal do Rio Grande do Sul, Rua Sarmento Leite 500, Porto Alegre, RS, CEP: 90050-170, Brazil. Tel.: +55-51-33083621; fax: +55-51-33083656.

E-mail address: belklein@ufrgs.br (A. Belló-Klein).

indicate that autophagy can be either beneficial or detrimental for the cell in the cardiac remodeling process.

The main strategy for reducing oxidative stress is to increase the endogenous antioxidant reserve [3]. Sulforaphane, an organosulfur compound found in cruciferous vegetables, such as broccoli sprouts, has the capacity to stimulate intracellular antioxidants and phase II detoxification enzymes [15,16] via activation of the Nrf-2-Keap-1-ARE signaling pathway [17]. In a mouse model of diabetic cardiomyopathy, sulforaphane was able to prevent pathological cardiac remodeling by decreasing oxidative stress and inflammation, which was associated with increased expression of superoxide dismutase (CuZn-SOD or Mn-SOD), catalase and heme oxygenase-1 (HO-1) [18]. Sulforaphane also improved cardiac function and protected the heart against ischemia–reperfusion injury and AIDS-induced cardiomyopathy, these effects being related to its capacity to reduce apoptosis [19–21]. Furthermore, Z. Zhang and colleagues (2014) demonstrated that sulforaphane attenuated oxidative stress and induced autophagy, preserving cardiac function in diabetic cardiomyopathy [22].

No studies to date have examined the role of sulforaphane in cardiac remodeling after myocardial infarction (MI). Thus, the aim of the present study was to test the hypothesis that treatment with sulforaphane could attenuate pathological cardiac remodeling post-infarction, by modulating oxidative stress, cell survival and cell death-related proteins.

2. Materials and methods

2.1. Animals and experimental design

Male Wistar rats (347 ± 18 g; *n* = 28 rats) were obtained from the Central Animal House of the Federal University of Rio Grande do Sul, Brazil. Rats were housed in plastic cages with free access to water and pelleted food, and they were maintained under standard laboratory conditions (temperature of 21°C, 12 h light/dark cycle). All animal

experiments were performed in accordance with the Institutional Animal Care Committee Guidelines. The animals were randomly divided into four groups: untreated sham (SHAM; *n* = 8), untreated acute MI (*n* = 8), sham treated with sulforaphane (SHAM + SFN, *n* = 7) and acute MI treated with sulforaphane (MI + SFN, *n* = 5). Initial cardiac function was measured by echocardiography at day 3 post sham and coronary artery ligation surgery. Subsequently, sulforaphane (R,S-sulforaphane; LKT Laboratories) was administered daily at a dose of 5 mg/kg, intraperitoneally, for 25 days. This dose of 5 mg is equivalent to 28 μmol of sulforaphane. Sulforaphane was prepared in 0.9% NaCl containing 0.5% (v/v) dimethyl sulfoxide. Untreated rats received the same solution without sulforaphane. Animals were monitored daily and their body weight was recorded every 3 days. At the end of the treatment period (28 days), cardiac function was measured by echocardiography prior to sacrificing animals and collecting their tissues for further analysis.

2.2. Surgical procedure for MI

MI was induced according to a previously described procedure [6,23]. Briefly, animals were anesthetized (ketamine 90 mg/kg plus xylazine 20 mg/kg, i.p.), intubated and ventilated via a tracheal cannula using a constant-volume rodent ventilator. Left thoracotomy was performed in the third intercostal space followed by pericardiotomy, without heart exteriorization. The left coronary artery was identified and permanently occluded with a 6.0 nylon monofilament suture. Subsequently, the thoracic cavity was closed and the pneumothorax was reduced by aspirating the existing air using a syringe, and the skin was sutured. Sham-operated rats were subjected to the same procedure without ligation of the coronary artery. Following surgery, an opioid analgesia (tramadol chlorhydrate – 5 mg/kg, 8–8 h, i.p.) was administered to the rats to relieve pain and discomfort. The mortality rate was approximately 10% at 24 h following the surgical procedure, not including additional deaths during the protocol period.

2.3. Echocardiographic analysis

For echocardiographic analysis, rats were anesthetized (ketamine 90 mg/kg plus xylazine 20 mg/kg, i.p.) and placed in the left lateral decubitus position to obtain cardiac images. Acquisition of echocardiographic images was achieved using a Philips HD7 XE ultrasound system with an L12–13 MHz transducer. Images were evaluated by an experienced operator, blinded to the experimental groups. Left ventricular end diastolic diameter (LVEDD, cm) and left ventricular end systolic diameter (LVESD, cm), left ventricular posterior wall thickness during diastole (LVPWD, cm) and left ventricular

Table 1
Morphometric, echocardiographic parameters and serum liver enzymes at 28 days after MI with and without sulforaphane treatment

Parameters	Untreated		Sulforaphane (SFN)	
	SHAM	MI	SHAM	MI
N	8	8	7	5
Morphometric data				
Final body weight (g)	380 ± 25	376 ± 19	397 ± 22	378 ± 20
Heart mass (g)	0.90 ± 0.05	1.02 ± 0.07 ^{#,a}	0.94 ± 0.03	1.03 ± 0.08 ^{#,c}
Heart mass/body weight (mg/g)	2.37 ± 0.18	2.71 ± 0.20 ^{#,a}	2.38 ± 0.13	2.73 ± 0.09 ^{#,c}
Liver wet/dry weight (g/g)	3.52 ± 0.07	3.61 ± 0.13	3.47 ± 0.07	3.50 ± 0.06
Lung wet/dry weight (g/g)	4.73 ± 0.10	4.67 ± 0.20	4.50 ± 0.13	4.60 ± 0.19
Echocardiographic data				
Infarct size (%)	–	55.3 ± 8.8	–	52.9 ± 7.5
HR (beats/min)	210 ± 17	227 ± 15	226 ± 20	211 ± 5
LVEDD (cm)	0.69 ± 0.04	0.87 ± 0.05 ^{#,a}	0.68 ± 0.05	0.84 ± 0.05 ^{#,c}
LVESD (cm)	0.33 ± 0.05	0.69 ± 0.06 ^{#,a}	0.32 ± 0.07	0.64 ± 0.05 ^{#,c}
LVPWD (cm)	0.17 ± 0.02	0.15 ± 0.04	0.16 ± 0.03	0.17 ± 0.03
LVPWS (cm)	0.28 ± 0.02	0.24 ± 0.05	0.29 ± 0.06	0.27 ± 0.04
Wall Tension Index	2.02 ± 0.17	2.92 ± 0.78 ^{#,a}	2.16 ± 0.50	2.41 ± 0.38 [#]
Ejection fraction (EF%)	51.6 ± 7.2	29.5 ± 4.5 ^{#,a}	52.1 ± 9.2	30.5 ± 4.8 ^{#,c}
FAC (%)	41.1 ± 9.0	18.1 ± 5.0 ^{#,a}	40.9 ± 9.0	21.5 ± 2.0 ^{#,c}
Peak E (cm/s)	129 ± 13	153 ± 20 [#]	129 ± 19	140 ± 32 [#]
Peak A (cm/s)	83 ± 11	60 ± 22 [#]	75 ± 8	76 ± 17 [#]
E/A ratio	1.56 ± 0.17	3.05 ± 1.65 [#]	1.71 ± 0.12	1.83 ± 0.03 [#]
Serum liver enzymes				
AST (U/L)	90.6 ± 22.5	86.4 ± 18.8	75.1 ± 7.3	94.8 ± 35.9
ALT (U/L)	49.4 ± 5.7	50.4 ± 7.7	39.4 ± 5.6 ^a	52.8 ± 8.3 ^c
ALP (U/L)	109.2 ± 28.1	144.4 ± 35.6 [#]	105.6 ± 27.9	163.2 ± 50.1 ^{#,c}

LVEDD, left ventricular end diastolic diameter; LVESD, left ventricular end systolic diameter; LVPWD, left ventricular posterior wall thickness at diastole; LVPWS, left ventricular posterior wall thickness at systole; FAC (%), fractional area change; AST, aspartate aminotransferase; ALT, alanine aminotransferase; ALP, alkaline phosphatase. Values expressed as mean ± SD.

[#] Significant difference between infarcted groups compared to sham groups (*P* < .05).

^a Significant difference from SHAM (*P* < .05).

^c Significant difference from SHAM + SFN (*P* < .05).

posterior wall thickness during systole (LVPWS, cm) and heart rate (beats/min) were measured using M-Mode in the basal, middle and apical planes, as previously described by our group and others [24–26]. Wall tension index was calculated as $WTI = LVEDD / 2 \times LVPWD$, to determine mechanical compensation. Also, left ventricular ejection fraction (EF%), calculated as $EF = (\text{end diastolic volume} - \text{end systolic volume} / \text{end diastolic volume}) \times 100$, and fractional area change (%), measured as $FAC = (\text{diastolic area} - \text{systolic area} / \text{diastolic area}) \times 100$, were used to determine contractile function and left ventricular systolic function, respectively [24]. Doppler was performed to assess peaks E and A. Infarct size (IS) was estimated as $IS = (I/EP) \times 100$, where I represents the measurement of the transverse plane of the arch corresponding to the segments with infarction and EP represents the total endocardial perimeter, measured at end diastole [25].

2.4. Morphometric analysis

Blood samples were collected under the influence of anesthesia, and rats were sacrificed by cervical dislocation. Heart, lungs and liver were rapidly excised and hearts were washed in phosphate buffer (PBS, pH 7.4) and weighed. For histological analysis, a slice of approximately 5 mm from the central portion of the heart was separated and immediately submerged in saturated Bouin's solution. The remaining viable cardiac muscle was immediately frozen in liquid nitrogen for biochemical and molecular biological analysis. Livers and lungs were blotted, weighed and then placed in a 60°C heating chamber until a stable dry weight was obtained. Cardiac hypertrophy was evaluated by calculating the ratio of heart weight (mg) to body weight (g). Liver and lung congestion were estimated by the ratio of wet to dry weight (g/g).

2.5. Serum liver enzymes

Blood was centrifuged (1000g, 10 min, 4°C), and serum was collected to measure liver enzymes, such as aspartate aminotransferase (AST) and alanine aminotransferase (ALT), according to the manufacturer's protocol using a kit purchased from Kovalent Ltda. and an alkaline phosphatase (ALP) kit purchased from Labtest Diagnóstica S.A. (Brazil).

2.6. Histological analysis for measurement of total collagen content

Transverse slices from the central portion of the heart (0.5 cm) were fixed in saturated Bouin's solution (12 h, room temperature), cryopreserved using sucrose solution (15% and 30%, 24 h each, 4°C) and sectioned in a cryostat (CM1850, Leica, Germany) (10 µm). Histological sections were stained with 0.1% Sirius Red (Direct Red 80, Sigma Aldrich), for 30 s at room temperature, washed once with water, counterstained with Harris hematoxylin (15 min, room temperature), dehydrated and covered with Canada balsam. In order to estimate cardiac collagen content, peri-infarction areas of histological sections were digitalized using a Olympus BX 50 microscope coupled to an Opton video camera and Image Pro Plus 6.0 software (Image Pro-Plus 6.1; Media Cybernetics, Silver Spring, USA). Estimation of percentage of the area occupied by cardiac muscle and collagen was made using the point counting method [27–29]. Histological images of the left ventricle from each animal were digitized and a point test system, composed by equidistant crosses, was laid over the images. When the upper right quadrant of the cross hits images of cardiac muscle, collagen or blood vessels were counted. The percentage area occupied by each tissue was obtained using the following equation:

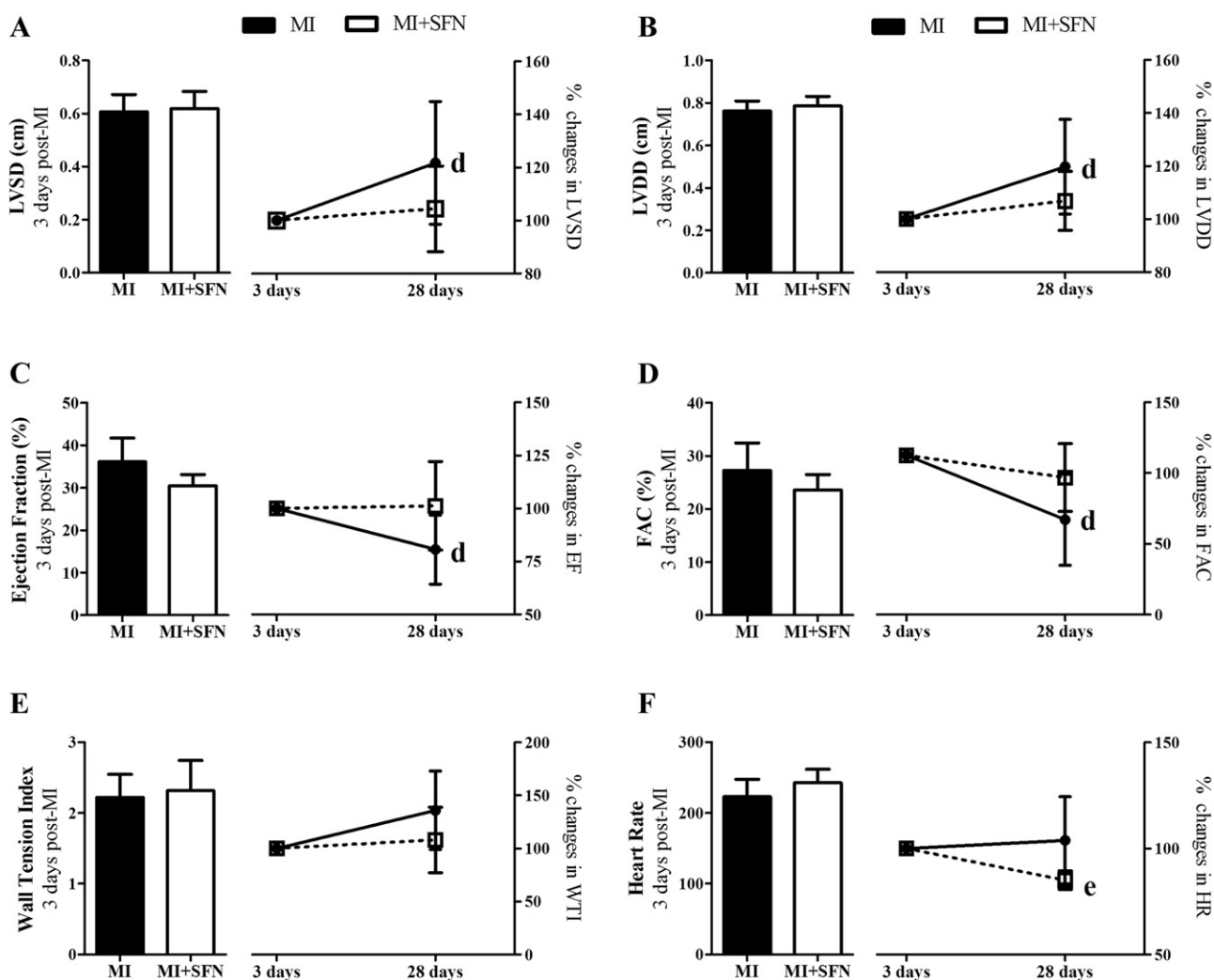


Fig. 1. Echocardiographic parameters at 3 days post-MI and percentage variation 28 days later (paired *t* test). Data collected at 3 days from both the MI and the MI + SFN groups were considered as 100%. Sulfuraphane (5 mg/kg/day) was administered at 3 days post-MI and continued for the duration of the study. (A) Left ventricle end systolic diameter; (B) left ventricle end diastolic diameter; (C) EF; (D) FAC; (E) wall tension index; (F) heart rate. Values are expressed as mean \pm SD from 5 to 8 animals per group. ^dSignificant difference between 28 days and 3 days in MI group (*P* < .05); ^esignificant difference between 28 days and 3 days in MI + SFN group (*P* < .05).

Percentage of area occupied by the tissue = (number of crosses counted in the tissue image/total number of crosses counted in the image) × 100. Crosses located in histological artifacts were not counted, as seen in Fig. 2.

2.7. Tissue preparation

For oxidative stress markers, cardiac tissues were homogenized in a solution containing 1.15% KCl + PMSF 1 mmol/L, using an Ultra-Turrax homogenizer. The suspension was centrifuged at 1000g for 10 min at 4°C, and the supernatant was used for analyses. For protein expression analyses, cardiac tissues were homogenized with Cell Lysis buffer (Cell Signaling Technology), according to the manufacturer's instructions.

2.8. Determination of protein concentration

Protein content was determined by the Lowry method and by DC Protein Assay (Bio-Rad), with bovine serum albumin as the standard.

2.9. Determination of antioxidant enzyme activity

Glutathione peroxidase (GPx) activity was estimated based on the consumption of NADPH and was measured spectrophotometrically at 340 nm. The activity was expressed as nanomoles of peroxide/hydroperoxide reduced per minute per milligram of protein [30]. Superoxide dismutase (SOD) activity was evaluated on the basis of the inhibition of the superoxide radical reaction with pyrogallol and was measured at 420 nm. It was expressed as units per milligram of protein [31]. Catalase activity was measured by following the decrease

in hydrogen peroxide (H₂O₂) absorbance at 240 nm. It was expressed as nanomoles of H₂O₂ reduced per minute per milligram of protein [32].

2.10. Protein expression analysis

Western blot was used to analyze the immunocontent of different proteins. Electrophoresis was performed in a 8–15% bis-acrylamide gels, according to the size of protein of interest, loading 30 µg of proteins in a minivertical gel system (Bio-Rad). Proteins were transferred to a PVDF membrane (Immobilon-P Transfer Membrane, Millipore) in a mini-transblot electrophoretic tank or Trans-Blot SD Semi-Dry Transfer Cell. Membranes were blocked in 5% nonfat milk prepared in TBS-T (Tris buffer saline – 20 mmol/L Tris, 137 mmol/L NaCl, pH 7.4, with 0.1% Tween-20). Membranes were probed overnight with the following primary antibodies, prepared in 5% milk TBS-T: CuZn-SOD, HO-1, Bax, Bcl-2, phospho-p38 (Thr180), p38, PGC-1, phospho-Akt 1/2/3 (Ser-473), Akt 1/2/3, xanthine oxidase and anti-β-actin, purchased from Santa Cruz Biotechnology; GPx, poly (ADP-ribose) polymerase (PARP) and 4-hydroxynonenal (4-HNE), purchased from Abcam; caspase-3, phospho-ERK 1/2 (Thr202/Tyr204), ERK 1/2, phospho-AMPK (Thr172), AMPK and LC3B, purchased from Cell Signaling; Mn-SOD (Millipore) and catalase (Sigma Aldrich). Bound primary antibodies were detected using anti-rabbit or anti-mouse horseradish peroxidase-conjugated secondary antibodies prepared in 5% milk TBS-T (1:1000–1:5000), incubated for 2 h at room temperature. Membranes were developed using a chemiluminescent reagent, and fluorescent images were captured using a ChemiDoc MP system (Bio-Rad). Data were expressed as mean optical densities as quantified using Quantity One software. β-Actin and Ponceau red stain was used as the loading control for normalization.

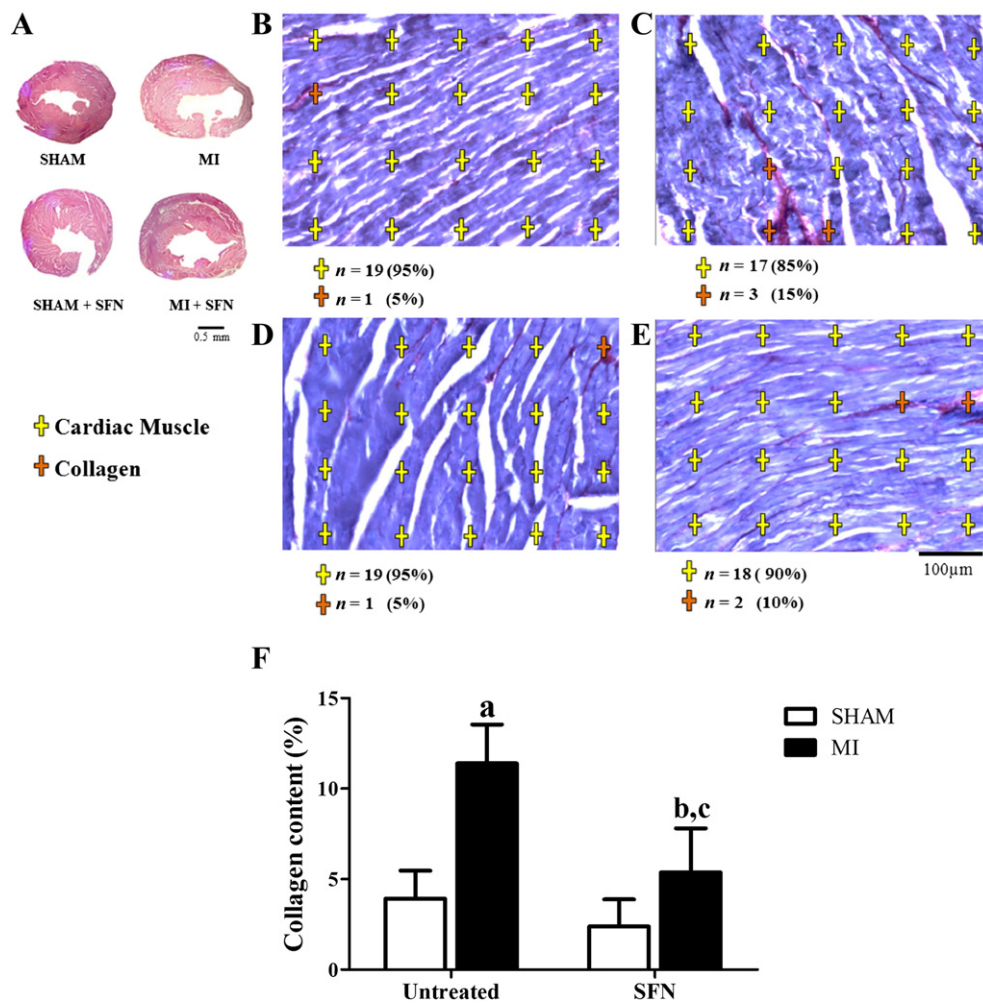


Fig. 2. Collagen content in the remaining viable cardiac tissue at 28 days post-MI with and without sulforaphane treatment (5 mg/kg/day). Representative transverse cardiac cross-section images from experimental groups of hearts at 28 days postinfarction (A); digitized images of cardiac tissue showing the percentage of muscle fibers and collagen (B–E). In these histological sections, cardiac muscle is stained in purple (yellow crosses) and collagen is stained in red (orange crosses); black crosses represent histological artifacts and were not counted (absent in the representative image). SHAM group (B); MI group (C); SHAM + SFN group (D); and MI + SFN group (E). Total collagen content in the remaining viable cardiac tissue, expressed in percentage (F). Values are expressed as mean ± SD from 5 to 8 animals per group. ^aSignificantly different from SHAM ($P < .05$); ^bSignificantly different from MI ($P < .05$); ^cSignificantly different from SHAM + SFN ($P < .05$).

2.11. Statistical analysis

Data were expressed as mean \pm SD. All results were analyzed using two-way ANOVA, except for the temporal cardiac function data that were analyzed by paired Student's *t* tests. Student–Newman–Keuls was used as a *post hoc* test. Values of $P < .05$ were considered statistically significant.

3. Results

3.1. Body weight and morphometric analysis

There was no statistical difference in the final body weight among the four groups at 28 days postsurgery (Table 1). Cardiac hypertrophy, as measured by heart weight-to-body weight ratio, was significantly increased in MI (14.3%, $P < .001$) and MI + SFN (14.7%, $P < .001$) compared to their respective control groups (Table 1). The lung and liver wet-to-dry weight ratios remained unchanged in the MI and MI + SFN groups compared to their respective control groups, indicating absence of lung and liver congestion (Table 1).

3.2. Liver function

Serum AST activity remained unchanged among groups. ALT levels remained unchanged in the untreated MI group compared to the SHAM group but was significantly increased in the MI + SFN group (33%, $P < .05$) compared with the SHAM + SFN group. Sulforaphane treatment was able to decrease ALT activity in the SHAM + SFN group (20%, $P < .05$) compared with the SHAM group (Table 1). There was an increase in ALP levels in the MI and MI + SFN groups compared with their respective SHAM groups, but the increase was significant only in MI + SFN compared with the SHAM + SFN group (Table 1).

3.3. Echocardiographic parameters

Table 1 shows echocardiographic measurements at 28 days post-MI. Infarct size did not differ between the MI ($57 \pm 9\%$) and MI + SFN ($52 \pm 8\%$) groups. MI induced cardiac dysfunction, which was shown by a significant increase in LVEDD and LVESD, and a significant decrease in ejection fraction (EF) and fractional area change (FAC) compared with the sham groups. Treatment with sulforaphane was unable to restore these parameters in the MI + SFN group compared with the respective untreated MI group (Table 1). Wall tension index increased significantly in the MI group (45%, $P < .01$) compared to the SHAM group (Table 1) but was modestly reduced (18%, nonsignificant) in the MI + SFN group compared to MI. E/A ratio was significantly higher in infarcted groups compared to sham groups ($P < .05$). However, there was no statistical difference between MI and MI + SFN groups (Table 1).

A time-course profile of the cardiac parameters in the MI and MI + SFN groups at day 3 and day 28 post-MI is shown in Fig. 1. On the first day, chamber diameters, contractility indexes and heart rate were not statistically different between groups, indicating homogeneity of the experimental model (Fig. 1, bars). However, as time progressed (Fig. 1, lines; considering each parameter as 100% at day 3), the MI group demonstrated a significant increase in LVESD (22%) and LVEDD (20%), a significant decrease in EF (20%) and FAC (24%) and a nonsignificant increase in wall tension index. This set of results indicates progressive worsening of cardiac dysfunction in the MI group. On the other hand, the MI + SFN group did not show a difference between these parameters at day 3 and day 28. Interestingly, the MI + SFN group demonstrated a significant reduction in heart rate at the end of day 28 compared with the measurements on day 3 (Fig. 1).

3.4. Histological analyses of total collagen content

Total collagen content in the viable myocardium, measured in the border area of the scar tissue, showed a significant increase (2.9-fold) in the MI group ($11.4 \pm 1.9\%$) compared with the SHAM group ($3.9 \pm 1.4\%$) ($P < .01$) (Fig. 2). Sulforaphane treatment significantly reduced the collagen content 2.1-fold in the MI + SFN group ($5.3 \pm 2.1\%$) compared with the MI group ($P < .001$) (Fig. 2). Positive correlation was observed between collagen content and E/A ratio ($P < .01$, $r = 0.63$).

3.5. Oxidative stress markers

Xanthine oxidase protein expression increased in both infarcted groups ($P < .001$) compared with the noninfarcted groups, and this increase reached 109% in the MI group ($P < .01$) and 117% in the MI + SFN group ($P < .01$) compared with their respective sham groups (Fig. 3A). 4-HNE protein adduct increased in both infarcted groups ($P < .01$) compared with noninfarcted groups, and a significant increase in the MI + SFN group compared to SHAM + SFN (41%, $P < .01$) was observed (Fig. 3B).

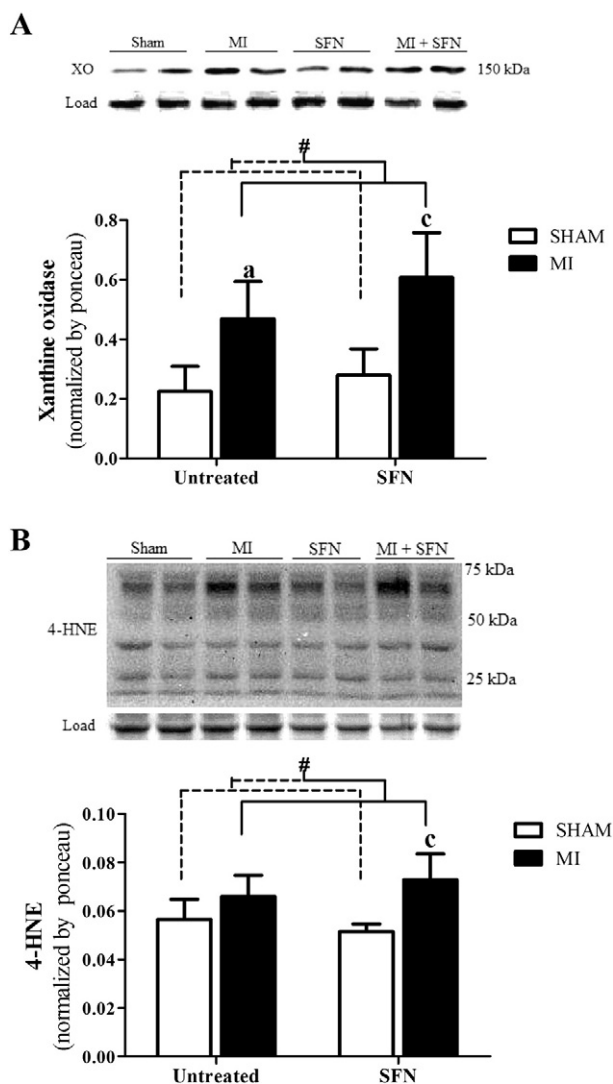


Fig. 3. Oxidative stress markers in cardiac tissue at 28 days post-MI with and without sulforaphane treatment (5 mg/kg/day). Xanthine oxidase (A) and 4-HNE (B). Values are expressed as mean \pm SD from 5 to 8 per group. #Significantly different between sham groups compared to infarcted groups ($P < .05$); *Significantly different from SHAM ($P < .05$); ^cSignificantly different from SHAM + SFN ($P < .05$).

Protein expression and enzyme activity of GPx were significantly increased in infarcted groups compared with sham groups ($P < .01$ and $P < .05$, respectively). Furthermore, the MI group presented a significant increase in GPx compared with the SHAM group (expression: 44%, $P < .01$; activity: 19%, $P < .01$, respectively) (Fig. 4A and B). Catalase protein expression and enzyme activity were not significantly altered among groups (Fig. 4C and D). Cytosolic superoxide dismutase (CuZn-SOD) expression increased in the MI (88%, $P < .05$) and SHAM + SFN (165%; $P < .001$) groups compared with the SHAM group (Fig. 4E); CuZn-SOD expression was maintained at an elevated level in the MI + SFN group (Fig. 4E). SOD enzymatic activity did not change among groups (Fig. 4F). Differences in Mn-SOD and transcription factor PGC-1 α protein expression were not statistically significant among groups (Fig. 4G and H).

Treatment with sulforaphane was able to increase HO-1 protein expression in both the SHAM + SFN (44%, $P < .01$) and MI + SFN (38.5%, $P < .01$) groups compared with untreated groups (Fig. 5).

3.6. Profile of MAPK signaling proteins

ERK 1/2 and p38 MAPK activities were assessed by measuring phosphorylated and total protein kinase isoforms. ERK 1/2 activity increased in the MI (46%, $P < .05$) and MI + SFN (82%, $P < .01$) groups compared with their respective sham groups (Fig. 6A). The increase observed in the MI + SFN group was 34% higher ($P < .01$) than in the MI group (Fig. 6A). p38 activity was increased only in the MI group (28%, $P < .01$) compared with the SHAM group (Fig. 6B). Sulforaphane treatment was able to decrease p38 protein expression (52%, $P < .01$) in the MI + SFN group compared with the MI group (Fig. 6B). A positive correlation was found between ERK activation and the oxidative markers xanthine oxidase ($P < .05$, $r = 0.31$) and 4-HNE ($P < .05$, $r = 0.42$), respectively (Fig. 6C and D). Akt activity increased in the MI + SFN group compared with the SHAM + SFN (30%, $P < .01$) and MI (35%, $P < .01$) groups, respectively (Fig. 6E).

3.7. Profile of apoptosis and autophagy-related proteins

Twenty-eight days postinfarction, proapoptotic Bax expression was found to be similar between the MI and the SHAM groups. Bax expression was significantly reduced in the SHAM + SFN group (33%, $P < .05$) compared with the SHAM group and in the MI + SFN group (35%, $P < .05$) compared with the MI group (Fig. 7A). Antiapoptotic Bcl-2 protein expression was also similar between the SHAM and the MI groups but was reduced in the SHAM + SFN (44%, $P < .05$) group compared to the SHAM group. Treatment with sulforaphane in the MI + SFN group was able to increase Bcl-2 levels (75%, $P < .05$) compared with the SHAM + SFN group (Fig. 7B). The Bax/Bcl-2 ratio was significantly reduced in the MI + SFN group compared with the MI group (44%, $P < .05$) and the SHAM + SFN group (53%; $P < .01$) (Fig. 7C). Caspase-3 protein expression was reduced in the MI + SFN group compared with the SHAM + SFN group (45%, $P < .05$) (Fig. 7D). PARP protein expression was not significantly different between groups (Fig. 7E).

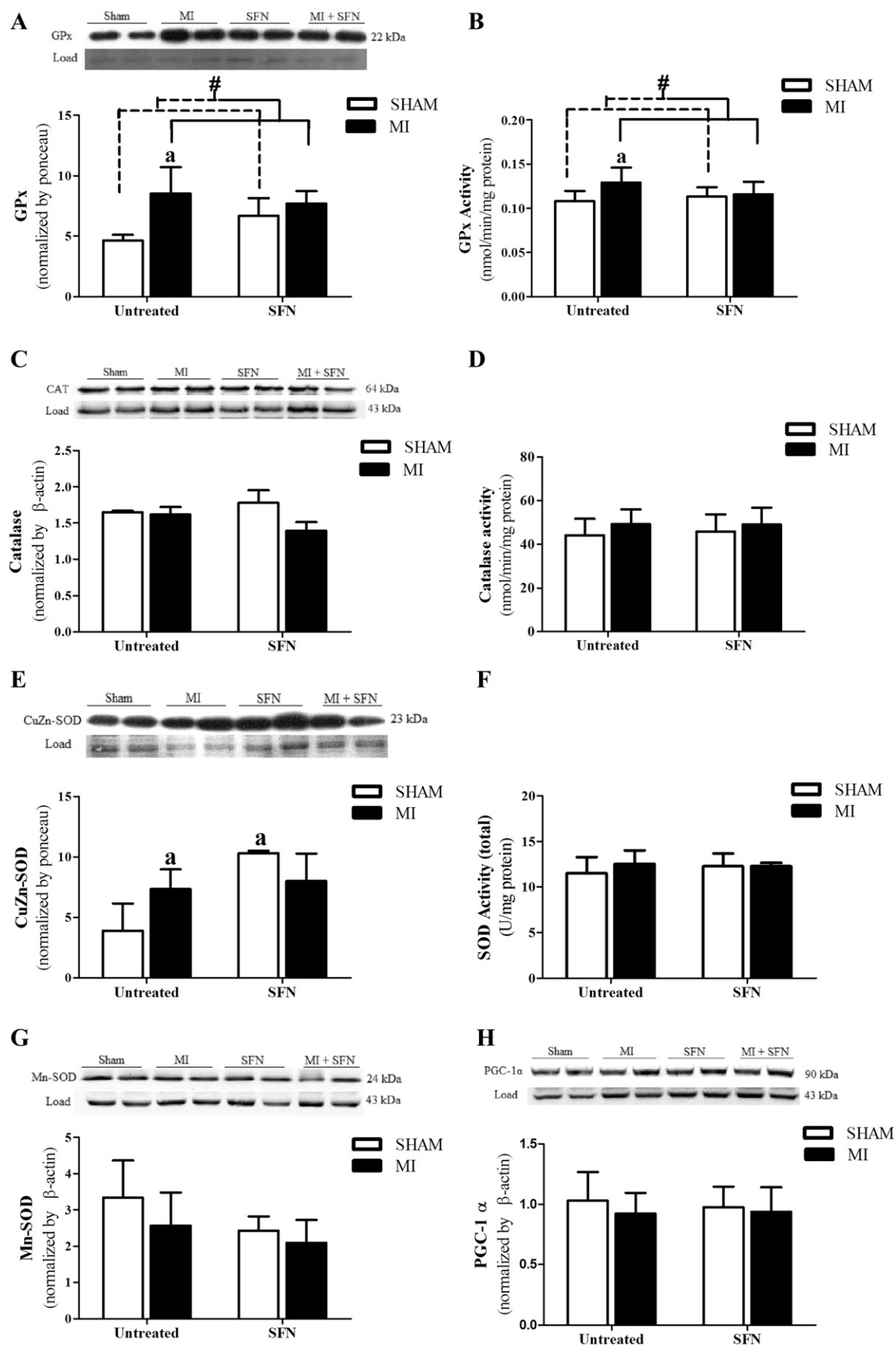
Autophagy-related signaling proteins were also measured. AMPK activity represented by the p-AMPK/AMPK ratio was reduced in infarcted groups compared with noninfarcted groups ($P < .05$). It was significantly decreased (33%; $P < .05$) in the MI group compared with the SHAM group (Fig. 8A). A similar pattern was observed for the LC3II/LC3I ratio, indicative that autophagy (Fig. 8B) was reduced in infarcted groups when compared with noninfarcted groups ($P < .01$). The LC3I/II ratio was significantly reduced in the MI group (33%, $P < .05$) compared with the SHAM group (Fig. 8B).

4. Discussion

The present study demonstrated that sulforaphane decreased fibrosis and cardiac dilation contributing to mitigation of the progression of cardiac dysfunction following MI in an *in vivo* model. Although sulforaphane was not able to reduce MI-induced oxidative stress, it caused an increase in HO-1 expression. These outcomes were associated with an up-regulation of components of survival pathways, such as ERK 1/2 and Akt, and down-regulation of death signaling proteins, such as p38 and Bax/Bcl-2-caspase-3.

The surgical procedure resulted in a mortality rate of approximately 28% in the first 24 h, and the cardiac function findings were similar to those previously described by our group [6,23]. The initial echocardiographic parameters at 3 days post-MI indicated a homogeneous model prior to therapeutic intervention. Sulforaphane was administered at 72 h post-MI based on previous studies highlighting its antiinflammatory properties [33,34]. Targeting inflammatory pathways in a timely manner can reduce cardiomyocyte injury and attenuate adverse cardiac remodeling, without interfering with the initial infarct healing phase [35,36]. Toxic effects of chronic administration of sulforaphane, as evaluated by AST and ALT activity, were not detected, as sham and treatment groups did not show significant differences. On the other hand, when evaluating ALP activity, some toxicity was observed only in the MI + SFN group.

In the present study, MI and MI + SFN rats developed cardiac hypertrophy and dysfunction, without overt signs of congestive heart failure (absence of lung and liver congestion). Sulforaphane was not able to reduce infarction-induced hypertrophy, as has been observed in cardiomyopathy experimental models, such as those for diabetes and isoproterenol [18,37]. This finding seems to be positive since, in the present study, attenuation of cardiac hypertrophy could represent an additional loss in contractile function, in hearts with approximately 52% of infarction area. Cardiac dysfunction, promoted by infarction, was evidenced by chamber dilation (increased LVEDD and LVESD) and reduced EF and FAC. However, wall tension index, which was increased only in the MI group, was not significantly altered in the MI + SFN group. Moreover, infarcted groups presented a significant increase in E/A ratio, indicating a restriction pattern during diastolic filling 4 weeks after infarction [24,38]. However, it can be observed lower values in MI + SFN compared to MI group. In a time-course echocardiographic analysis of the infarcted groups, comparing the pretreatment (3 day) and posttreatment (28 day) periods, the MI group presented a significant worsening in all parameters related to ventricular chamber dilation and contractile function. On the other hand, these parameters remained constant in the MI + SFN group comparing the third day to the twenty-eighth day. These data showed that sulforaphane caused a slower evolution of cardiac dysfunction, evidenced by diminished percentage variation in pathological cardiac remodeling. Piao and colleagues (2010) showed that sulforaphane was able to improve cardiac function after ischemia–reperfusion injury (an *ex vivo* model) [19]. Results from our group have also shown that pretreatment with a low dose of sulforaphane (0.5 mg/kg, i.p.) improved cardiac contractility after ischemia–reperfusion injury (data not published). This improvement was not observed when a high dose of sulforaphane (10 mg/kg, i.p.) was used in the same ischemia–reperfusion protocol [39]. Moreover, the MI + SFN group presented reduced fibrosis compared with the MI group. Fibrosis has been considered an important target to control pathological cardiac remodeling [2,40]. Sulforaphane has been shown to reduce fibrosis in diabetic cardiomyopathy, which was associated with preserved cardiac function [18,22]. Furthermore, some clinical trials have also demonstrated that reduction of fibrosis can improve cardiac function [41]. Moreover, significant positive correlation was observed between E/A ratio and fibrosis, both markers associated to diastolic dysfunction [42]. It suggests that the decreased collagen content in sulforaphane



treated group may contribute to preserve diastolic function. Anti-fibrotic activity after sulforaphane treatment has also been described in lung and skeletal muscle [43,44]. These data suggest that sulforaphane intervention may play an important role in attenuating cardiac remodeling during the course of the disease.

When analyzing oxidative markers, it was observed that infarction induced an increase in xanthine oxidase levels. This enzyme is implicated in the etiology of heart failure, supplying superoxide radicals. Xanthine oxidase expression is increased only in failing hearts but not in hypertrophic ventricles post-MI, suggesting its potential role in the transition from cardiac hypertrophy into failure [45]. In parallel, increased lipid peroxidation was observed in the MI and MI + SFN groups, as evaluated by the 4-HNE protein adduct, indicating lipid oxidative damage, which was not reduced by sulforaphane. This increased oxidative damage in both infarcted groups may stimulate antioxidant defenses, observed as increased levels of GPx and CuZn-SOD. This increased antioxidant response may have contributed to the maintenance of compensated cardiac hypertrophy observed in the infarcted groups 28 days post-MI. In fact, it has been reported that diminished antioxidant defenses are related to the progression of heart failure [46–48]. Also, overexpression of GPx prevents pathological cardiac remodeling after MI in mice [49]. Moreover, only sulforaphane treated groups presented increased expression of HO-1, indicating that stimulation of this enzyme may have contributed to mitigate the cardiac remodeling process observed in the MI + SFN group. Overexpression of HO-1 is reported to be cardioprotective and antiapoptotic in pathological cardiac remodeling [50]. By-products of HO-1 activity, such as carbon monoxide and biliverdin, have been considered responsible for its cytoprotective, antiapoptotic, antiinflammatory and antioxidant effects [51,52]. An increase in HO-1 may also contribute to antioxidant effects, promoting a shift to a more reduced redox condition. HO-1 has been shown to be modulated by transcription factors, such as PGC-1 α [22,53]. PGC-1 α plays an important role in the modulation of mitochondrial antioxidant enzymes and protects the heart against oxidative stress in a model of transverse aortic constriction [54]. In the present study, there was no difference in PGC-1 α expression after MI and sulforaphane intervention. Corroborating this finding, Mn-SOD expression, a downstream target for PGC-1 α , was also not altered. These results indicate that chronic treatment with sulforaphane stimulated HO-1 in the cardiac tissue but was not able to modulate mitochondrial antioxidant defenses via PGC-1 α in the remaining cardiac tissue postinfarction.

Redox-sensitive MAPK pathways showed a dynamic balance between ERK 1/2 and p38 in both infarcted groups. An increased activation of both ERK 1/2 and p38 kinases was observed in the MI group, whereas the MI + SFN group showed a higher ERK 1/2 activation, followed by a reduction in p38 activity. ERK 1/2 signaling is considered cardioprotective and is associated with compensated hypertrophy and survival [10]. In the present study, a significant correlation between oxidative markers and ERK 1/2 activation was observed. 4-HNE, besides being an end product of lipid peroxidation, is known to regulate MAPKs by a redox-dependent mechanism [55,56]. An increase in 4-HNE could represent a moderate stimulus capable of promoting an adaptive hormetic response [57], through ERK 1/2 activation. ROS generated by xanthine oxidase may also modulate ERK 1/2 activation. It has been demonstrated that xanthine oxidase phosphorylates ERK 1/2 in neonatal rat cardiomyocytes [58]. In the same way, sulforaphane caused an increase in Akt, another important prosurvival protein [59], in a group under stress conditions. Moreover, ERK 1/2 activation can contribute to increasing the expression of HO-1

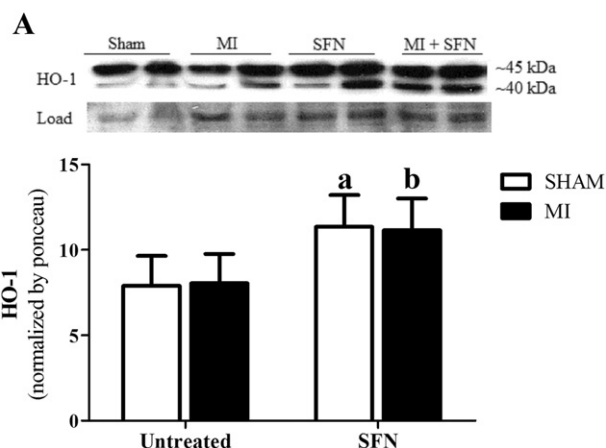


Fig. 5. Protein expression of HO-1 in cardiac tissue at 28 days post-MI with and without sulforaphane treatment (5 mg/kg/day). Ponceau red was used as loading control. Values are expressed as mean \pm SD from 4 animals per group. ^aSignificant difference from SHAM ($P < .05$); ^bsignificant difference from MI ($P < .05$).

[60], favoring cardioprotective effects, as well as to reducing the Bax/Bcl-2 ratio, decreasing proapoptosis signaling [51]. E. Leoncini and colleagues (2011) demonstrated that ERK 1/2 is involved in the sulforaphane cytoprotection of H₂O₂-induced cell death in cardiomyocytes [61]. Apoptosis, maladaptive hypertrophy and fibrosis are associated with p38 signaling [62]. Although both kinases are redox sensitive, p38, also known as stress activated-protein kinase, is activated by a more oxidized condition, such as that observed in MI [10,23]. In fact, in the present study, p38 activation was associated with increased oxidative stress in the MI group. Our data suggest that sulforaphane can modulate a favorable crosstalk between ERK-Akt/p38 in the viable myocardium, contributing to the attenuation of cardiac dysfunction observed in the MI + SFN group.

Apoptosis-related proteins were also investigated in the present study. Although there was no difference in apoptosis signaling in the MI group compared to the SHAM group, contributing to our interpretation that the hearts were in a compensated phase, sulforaphane-treated groups presented low levels of proapoptotic Bax protein. Moreover, sulforaphane was able to stimulate Bcl-2 expression in the MI + SFN group, which led to a significant reduction in the Bax/Bcl-2 ratio. Caspase-3 was modestly reduced in the MI + SFN group compared to the MI group. A decrease in Bax and caspase-3 caused by sulforaphane has been reported in different experimental models of cardiac injury induced by ischemia–reperfusion and AIDS infection [19,21,22]. Another marker of apoptosis, cleaved PARP, which is related to DNA oxidative damage [48,63], was also measured and it remained unchanged in all groups. These findings demonstrated that sulforaphane down-regulated apoptosis-related proteins after MI, which may contribute to some protective effect against cell death.

Autophagy also contributes to cardiac cell death and pathological cardiac remodeling. To investigate if sulforaphane could modulate this process, phosphorylation of AMPK, an upstream kinase that activates autophagy, was quantified and the LC3II/LC3I ratio, an indicator of autophagosome formation [26], was determined. A significant decrease in AMPK phosphorylation and LC3II/I ratio was observed in both infarcted groups, indicating a reduction in autophagy. A possible mechanism for the reduction in AMPK that was observed in both the

Fig. 4. Enzymatic antioxidant defense in cardiac tissue at 28 days post-MI with and without sulforaphane treatment (5 mg/kg/day). Protein expression and enzyme activity of GPx (A and B), catalase (C and D) and SOD (E–G). Protein expression of transcription cofactor PGC-1 α (H). β -Actin and Ponceau red were used as loading control. Western blot analysis from 4 animals per group. Antioxidant enzyme activity from 5 to 8 animals per group. Values are expressed as mean \pm SD. ^aSignificantly different between sham groups compared to infarcted groups ($P < .05$); ^bsignificantly different from SHAM ($P < .05$).

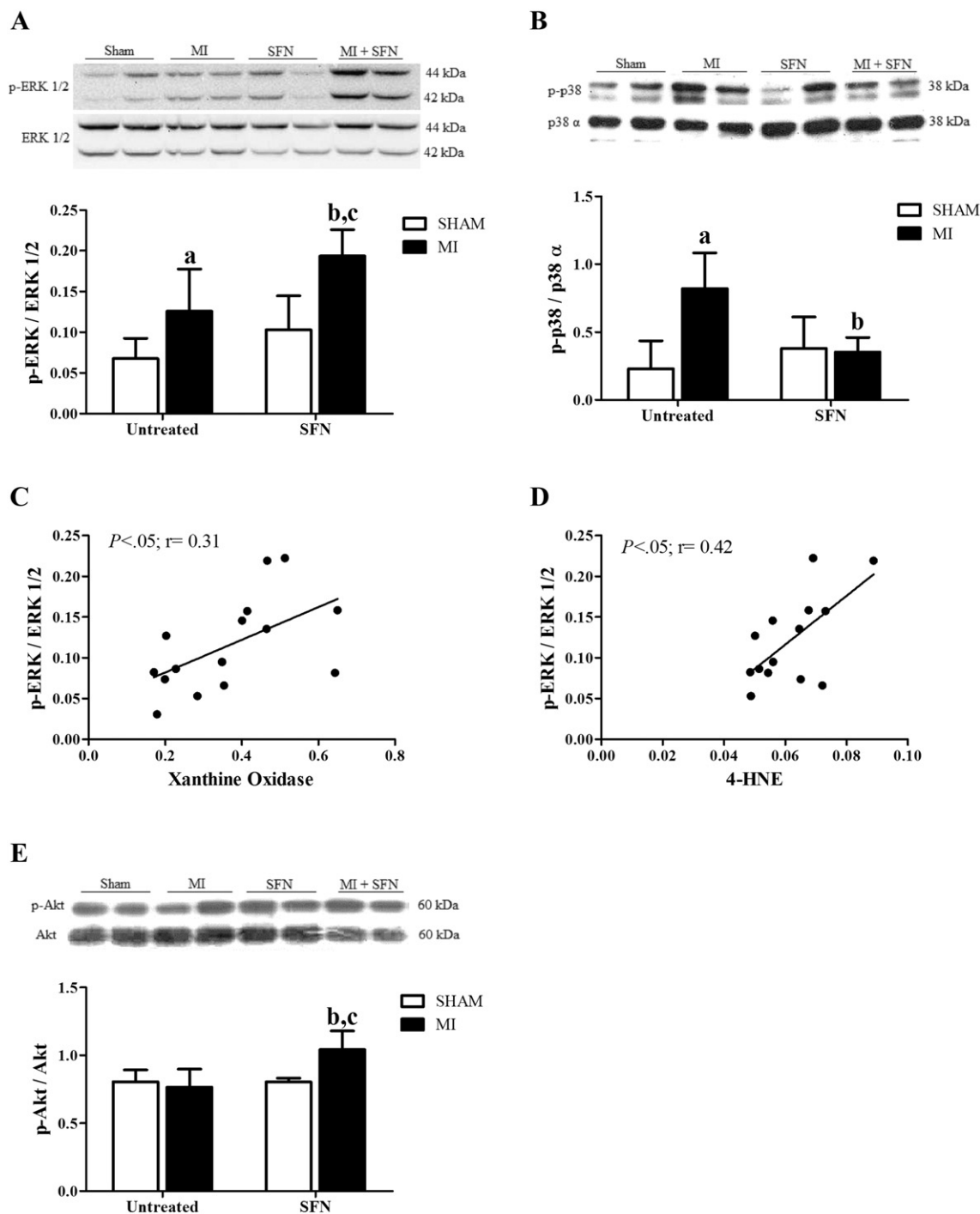


Fig. 6. Survival- and death-related protein kinases and correlation with oxidative stress in cardiac tissue at 28 days post-MI with and without sulforaphane treatment (5 mg/kg/day). ERK 1/2 activity (p-ERK/ERK 1/2) (A), p38 activity (p-p38/p38α) (B), correlation of ERK 1/2 activity and xanthine oxidase (C) and Akt activity (p-Akt/Akt) (E). Ponceau red were used as loading control. Values are expressed as mean \pm SD from 5 to 6 animals per group. *Significantly different from SHAM ($P < .05$); ^asignificantly different from MI ($P < .05$); ^bsignificantly different from SHAM + SFN ($P < .05$).

MI and MI + SFN groups could be due to ERK 1/2 activation. In human leukemia cells, it was demonstrated that ERK phosphorylation preceded AMPK dephosphorylation, suggesting an inhibitory effect [64]. Perhaps the reduction in autophagy could be contributing to maintenance of a stable phase of cardiac hypertrophy. H. Zhu and colleagues (2007) demonstrated that reduction of autophagy in a model of hemodynamic stress was associated with diminished pathological remodeling [14]. In a model of diabetic cardiomyopathy,

sulforaphane was able to maintain AMPK and LC3II/I at similar levels to the control group, improving cardiac function [22]. The data obtained in the present study show that sulforaphane was not able to modulate the autophagy process in this period postinfarction. Therefore, more studies in different post-MI periods should be conducted to determine whether sulforaphane can contribute to this process.

A limitation of the present study was the lack of more markers regarding to extracellular matrix, in order to strength the preliminary

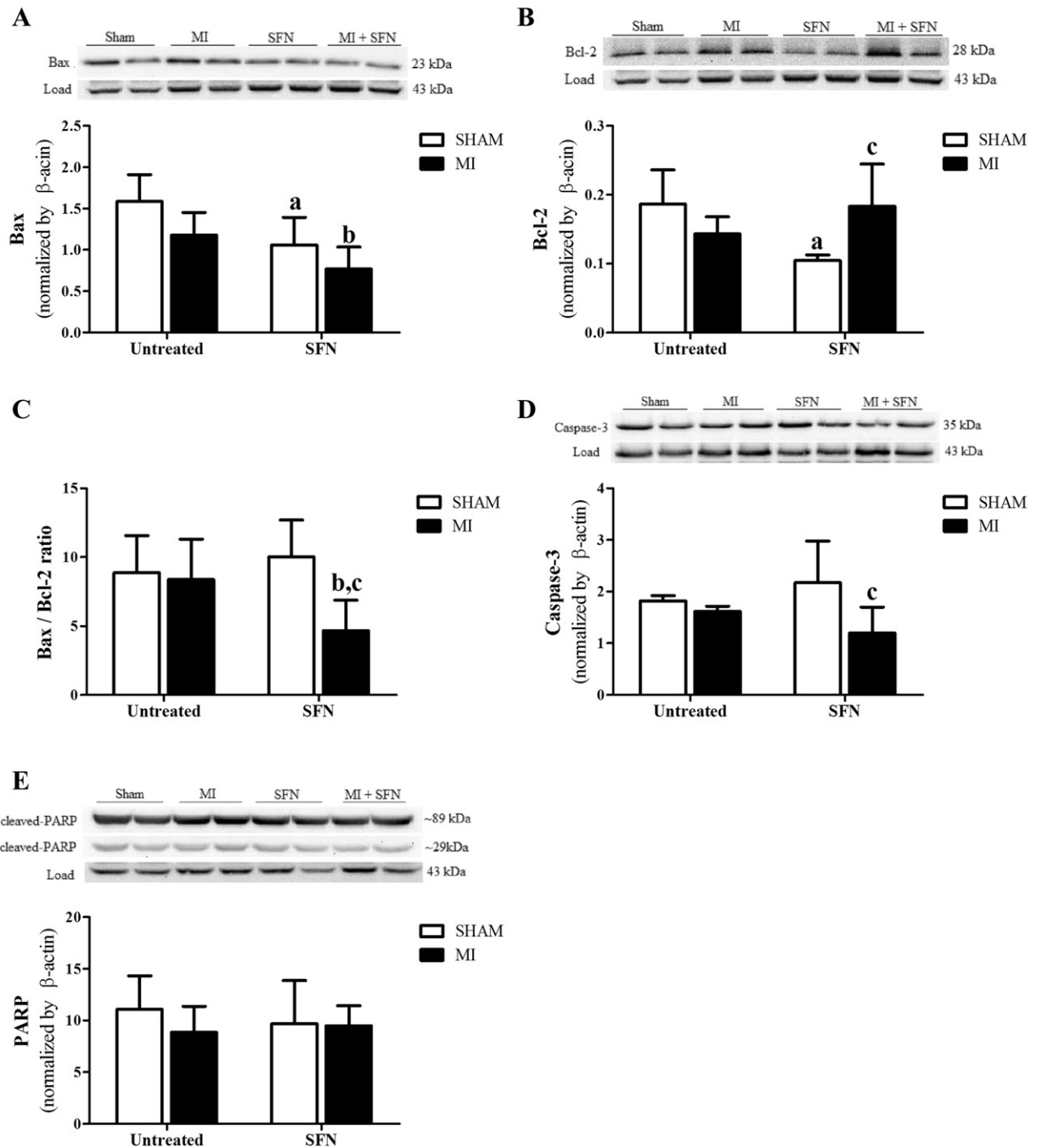


Fig. 7. Apoptosis-related proteins Bax (A), Bcl-2 (B), Bax/Bcl-2 ratio (C), caspase-3 (D) and PARP (E) protein expression in cardiac tissue at 28 days post-MI with or without sulforaphane (5 mg/kg/day) treatment. β -Actin was used as loading control. Values are expressed as mean \pm SD from 4 to 5 animals per group. ^aSignificantly different from SHAM ($P < .05$); ^bsignificantly different from MI ($P < .05$); ^csignificantly different from SHAM + SFN ($P < .05$).

data of collagen content, as well as biomarkers of inflammation, another key mechanism involved in the cardiac remodeling [65]. It has been well demonstrated that sulforaphane presents antiinflammatory effects on cardiac tissue and carotid artery [22,44,66], suggesting that sulforaphane can also contribute to mitigate cardiac remodeling by modulation of the inflammatory system.

In conclusion, sulforaphane increased HO-1, which may generate a redox environment favorable to the activation of prosurvival and deactivation prodeath pathways in the cardiac tissue (Fig. 9). This natural compound attenuated the fibrotic process, which may contribute to mitigate the progression of cardiac remodeling postinfarction.

Conflicts of interest

None.

Acknowledgments

This work was supported by Brazilian Research Agencies: Conselho Nacional de Desenvolvimento Científico e Tecnológico (CNPq), Coordenação de Aperfeiçoamento de Pessoal de Nível Superior – Program CAPES-DFAIT and Fundação de Amparo à Pesquisa do Rio

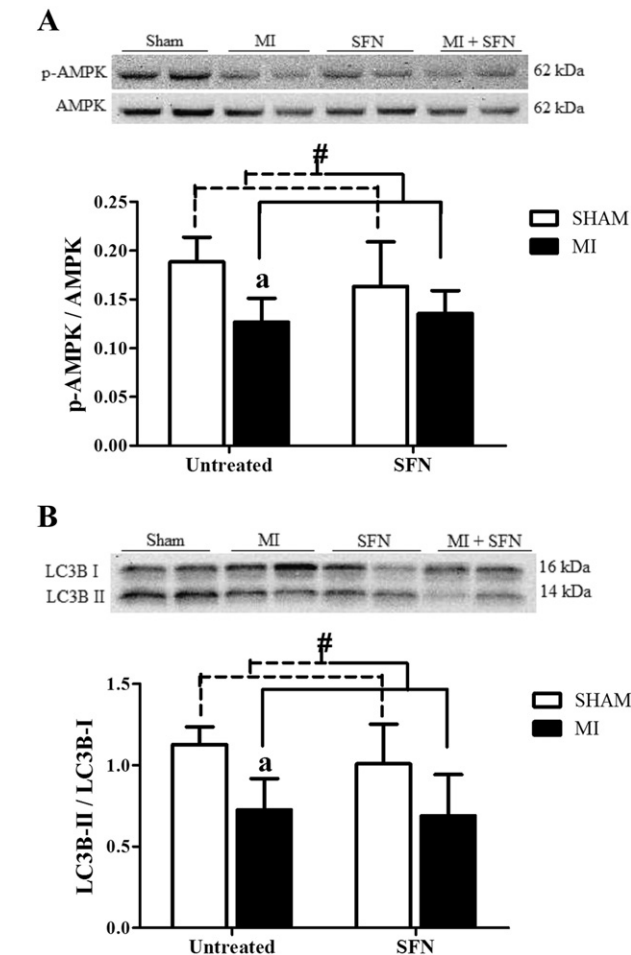


Fig. 8. Autophagy-related proteins AMPK (p-AMPK α /AMPK α) (A) and LC3B (LC3BII/LC3BI) (B) protein expression in cardiac tissue at 28 days post-MI with or without treatment with sulforaphane (5 mg/kg/day). β -Actin was used as loading control. Values are expressed as mean \pm SD from 4 animals per group. Values are expressed as mean \pm SD from 5 to 8 animals per group. *Significantly different between infarcted groups compared to sham groups ($P < .05$); #significantly different from SHAM ($P < .05$).

Grande do Sul (FAPERGS), as well as Northern Ontario School of Medicine. Technical assistance from Tânia Fernandes and Heidi Forsyth is greatly acknowledged. Rafael Fernandes and Jéssica Bonetto were exchange students, under the Canada–Brazil training program. Dr. Pawan Singal is the holder of the Dr. Naranjan S. Dhalla Chair in Cardiovascular Research supported by St. Boniface Hospital Research Foundation.

References

- [1] Opie LH, Commerford PJ, Gersh BJ, Pfeffer MA. Controversies in ventricular remodelling. *Lancet* 2006;367:356–67.
- [2] González A, Ravassa S, Beaumont J, López B, Díez J. New targets to treat the structural remodeling of the myocardium. *J Am Coll Cardiol* 2011;58:1833–43.
- [3] Hori M, Nishida K. Oxidative stress and left ventricular remodelling after myocardial infarction. *Cardiovasc Res* 2009;81:457–64.
- [4] Khaper N, Singal PK. Modulation of oxidative stress by a selective inhibition of angiotensin II type 1 receptors in MI rats. *J Am Coll Cardiol* 2001;37:1461–6.
- [5] Hill MF, Palace VP, Kaur K, Kumar D, Khaper N, Singal PK. Reduction in oxidative stress and modulation of heart failure subsequent to myocardial infarction in rats. *Exp Clin Cardiol* 2005;10:146–53.
- [6] de Castro AL, Tavares AV, Campos C, Fernandes RO, Siqueira R, Conzatti A, et al. Cardioprotective effects of thyroid hormones in a rat model of myocardial infarction are associated with oxidative stress reduction. *Mol Cell Endocrinol* 2014;391:22–9.
- [7] Dorn GW. Apoptotic and non-apoptotic programmed cardiomyocyte death in ventricular remodelling. *Cardiovasc Res* 2009;81:465–73.
- [8] Chung SD, Lai TY, Chien CT, Yu HJ. Activating Nrf-2 signaling depresses unilateral ureteral obstruction-evoked mitochondrial stress-related autophagy, apoptosis and pyroptosis in kidney. *PLoS One* 2012;7, e47299.
- [9] Essick EE, Wilson RM, Pimentel DR, Shimano M, Baid S, Ouchi N, et al. Adiponectin modulates oxidative stress-induced autophagy in cardiomyocytes. *PLoS One* 2013;8, e68697.
- [10] Qin F, Liang MC, Liang CS. Progressive left ventricular remodeling, myocyte apoptosis, and protein signaling cascades after myocardial infarction in rabbits. *Biochim Biophys Acta* 1740;2005:499–513.
- [11] Baldi A, Abbate A, Bussani R, Patti G, Melfi R, Angelini A, et al. Apoptosis and post-infarction left ventricular remodeling. *J Mol Cell Cardiol* 2002;34:165–74.
- [12] Rothermel BA, Hill JA. Autophagy in load-induced heart disease. *Circ Res* 2008;103:1363–9.
- [13] Lavandro S, Troncoso R, Rothermel BA, Martinet W, Sadoshima J, Hill JA. Cardiovascular autophagy: concepts, controversies, and perspectives. *Autophagy* 2013;9:1455–66.
- [14] Zhu H, Tannous P, Johnstone JL, Kong Y, Shelton JM, Richardson JA, et al. Cardiac autophagy is a maladaptive response to hemodynamic stress. *J Clin Invest* 2007;117:1782–93.

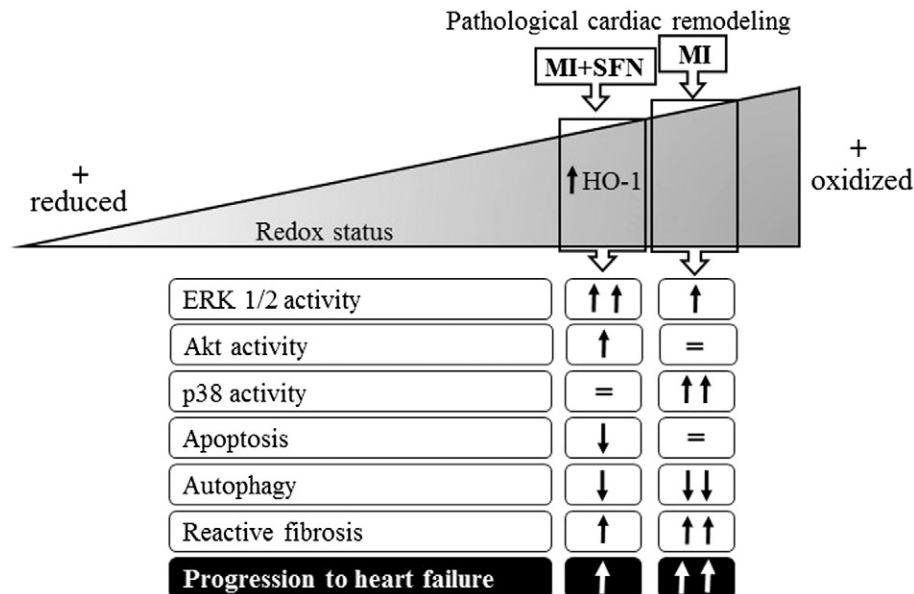


Fig. 9. Schematic illustration summarizing the effects of sulforaphane on markers of oxidative stress, apoptosis, fibrosis, autophagy and the relevant downstream signaling components 28 days post-MI. Symbols: ↑, increase activity or levels; ↓, decreased activity or levels; =, unchanged activity or levels compared to noninfarcted control rats.

- [15] Angeloni C, Leoncini E, Malaguti M, Angelini S, Hrelia P, Hrelia S. Modulation of phase II enzymes by sulforaphane: implications for its cardioprotective potential. *J Agric Food Chem* 2009;57:5615–22.
- [16] Fahey JW, Talalay P. Antioxidant functions of sulforaphane: a potent inducer of phase II detoxication enzymes. *Food Chem Toxicol* 1999;37:973–9.
- [17] Bai Y, Wang X, Zhao S, Ma C, Cui J, Zheng Y. Sulforaphane protects against cardiovascular disease via Nrf2 activation. *Oxid Med Cell Longev* 2015;2015:407580.
- [18] Bai Y, Cui W, Xin Y, Miao X, Barati MT, Zhang C, et al. Prevention by sulforaphane of diabetic cardiomyopathy is associated with up-regulation of Nrf2 expression and transcription activation. *J Mol Cell Cardiol* 2013;57:82–95.
- [19] Piao CS, Gao S, Lee GH, Kim DS, Park BH, Chae SW, et al. Sulforaphane protects ischemic injury of hearts through antioxidant pathway and mitochondrial K(ATP) channels. *Pharmacol Res* 2010;61:342–8.
- [20] Li Z, Galli U, Becker LE, Bruns H, Nickolgh A, Hoffmann K, et al. Sulforaphane protects hearts from early injury after experimental transplantation. *Ann Transplant* 2013;18:558–66.
- [21] Ho JN, Yoon HG, Park CS, Kim S, Jun W, Choue R, et al. Isothiocyanates ameliorate the symptom of heart dysfunction and mortality in a murine AIDS model by inhibiting apoptosis in the left ventricle. *J Med Food* 2012;15:781–7.
- [22] Zhang Z, Wang S, Zhou S, Yan X, Wang Y, Chen J, et al. Sulforaphane prevents the development of cardiomyopathy in type 2 diabetic mice probably by reversing oxidative stress-induced inhibition of LKB1/AMPK pathway. *J Mol Cell Cardiol* 2014;77:42–52.
- [23] Schenkel PC, Tavares AM, Fernandes RO, Diniz GP, Bertagnolli M, da Rosa Araujo AS, et al. Redox-sensitive pro-survival and proapoptotic protein expression in the myocardial remodeling post-infarction in rats. *Mol Cell Biochem* 2010;341:1–8.
- [24] Nozawa E, Kanashiro RM, Murad N, Carvalho AC, Cravo SL, Campos O, et al. Performance of two-dimensional Doppler echocardiography for the assessment of infarct size and left ventricular function in rats. *Braz J Med Biol Res* 2006;39:687–95.
- [25] Tavares AM, da Rosa Araújo AS, Baldo G, Matte U, Khaper N, Belló-Klein A, et al. Bone marrow derived cells decrease inflammation but not oxidative stress in an experimental model of acute myocardial infarction. *Life Sci* 2010;87:699–706.
- [26] Kabeya Y, Mizushima N, Ueno T, Yamamoto A, Kirisako T, Noda T, et al. LC3, a mammalian homologue of yeast Apg8p, is localized in autophagosome membranes after processing. *EMBO J* 2000;19:5720–8.
- [27] Zacharová G, Kubínová L. Stereological methods based on point counting and unbiased counting frames for two-dimensional measurements in muscles: comparison with manual and image analysis methods. *J Muscle Res Cell Motil* 1995;16:295–302.
- [28] Rodrigues FS, Souza MA, Magni DV, Ferreira AP, Mota BC, Cardoso AM, et al. N-Acetylcysteine prevents spatial memory impairment induced by chronic early postnatal glutaric acid and lipopolysaccharide in rat pups. *PLoS One* 2013;8:e78332.
- [29] Weibel E. Stereological methods. Practical methods for biological morphometry. London Academic Press; 1979 [ed.].
- [30] Flohé L, Günzler WA. Assays of glutathione peroxidase. *Methods Enzymol* 1984;105:114–21.
- [31] Marklund SL. Handbook of methods for oxygen radical research. CRC Press, Boca Raton - FL; 1985 243–7.
- [32] Aebi H. Catalase *in vitro*. *Methods Enzymol* 1984;105:121–6.
- [33] Nguyen B, Luong L, Naase H, Vives M, Jakaj G, Finch J, et al. Sulforaphane pretreatment prevents systemic inflammation and renal injury in response to cardiopulmonary bypass. *J Thorac Cardiovasc Surg* 2014;148:690–697.e3.
- [34] Nallasamy K, Jayashree M, Singhi S, Bansal A. Low-dose vs standard-dose insulin in pediatric diabetic ketoacidosis: a randomized clinical trial. *JAMA Pediatr* 2014;168:999–1005.
- [35] Hammerman H, Kloner RA, Schoen FJ, Brown EJ, Hale S, Braunwald E. Indomethacin-induced scar thinning after experimental myocardial infarction. *Circulation* 1983;67:1290–5.
- [36] Frangogiannis NG. The immune system and cardiac repair. *Pharmacol Res* 2008;58:88–111.
- [37] Kee HJ, Kim GR, Kim IK, Jeong MH. Sulforaphane suppresses cardiac hypertrophy by inhibiting GATA4/GATA6 expression and MAPK signaling pathways. *Mol Nutr Food Res* 2015;59:221–30.
- [38] Miranda A, Costa-e-Sousa RH, Werneck-de-Castro JP, Mattos EC, Olivares EL, Ribeiro VP, et al. Time course of echocardiographic and electrocardiographic parameters in myocardial infarct in rats. *An Acad Bras Cienc* 2007;79:639–48.
- [39] Bonetto JH, Fernandes RO, Seolin B, Müller D, Teixeira R, Araujo A, et al. Sulforaphane improves oxidative status without attenuating the inflammatory response or cardiac impairment induced by ischemia-reperfusion in rats. *Can J Physiol Pharmacol* 2016;94:508–16.
- [40] Burchfield JS, Xie M, Hill JA. Pathological ventricular remodeling: mechanisms: part 1 of 2. *Circulation* 2013;128:388–400.
- [41] Brilla CG. Regression of myocardial fibrosis in hypertensive heart disease: diverse effects of various antihypertensive drugs. *Cardiovasc Res* 2000;46:324–31.
- [42] Galderisi M. Diastolic dysfunction and diastolic heart failure: diagnostic, prognostic and therapeutic aspects. *Cardiovasc Ultrasound* 2005;3:9.
- [43] Artaud-Macari E, Goven D, Brayer S, Hamimi A, Besnard V, Marchal-Somme J, et al. Nuclear factor erythroid 2-related factor 2 nuclear translocation induces myofibroblastic dedifferentiation in idiopathic pulmonary fibrosis. *Antioxid Redox Signal* 2013;18:66–79.
- [44] Sun C, Li S, Li D. Sulforaphane mitigates muscle fibrosis in mdx mice via Nrf2-mediated inhibition of TGF-β/Smad signaling. *J Appl Physiol* 2016;120:377–90.
- [45] de Jong JW, Schoemaker RG, de Jonge R, Bernocchi P, Keijzer E, Harrison R, et al. Enhanced expression and activity of xanthine oxidoreductase in the failing heart. *J Mol Cell Cardiol* 2000;32:2083–9.
- [46] Khaper N, Kaur K, Li T, Farahmand F, Singal PK. Antioxidant enzyme gene expression in congestive heart failure following myocardial infarction. *Mol Cell Biochem* 2003;251:9–15.
- [47] Araujo AS, Ribeiro MF, Enzeveler A, Schenkel P, Fernandes TR, Partata WA, et al. Myocardial antioxidant enzyme activities and concentration and glutathione metabolism in experimental hyperthyroidism. *Mol Cell Endocrinol* 2006;249:133–9.
- [48] Wang J, Hao L, Wang Y, Qin W, Wang X, Zhao T, et al. Inhibition of poly (ADP-ribose) polymerase and inducible nitric oxide synthase protects against ischemic myocardial damage by reduction of apoptosis. *Mol Med Rep* 2015;11:1768–76.
- [49] Shiomi T, Tsutsui H, Matsusaka H, Murakami K, Hayashidani S, Ikeuchi M, et al. Overexpression of glutathione peroxidase prevents left ventricular remodeling and failure after myocardial infarction in mice. *Circulation* 2004;109:544–9.
- [50] Wang G, Hamid T, Keith RJ, Zhou G, Partridge CR, Xiang X, et al. Cardioprotective and antiapoptotic effects of heme oxygenase-1 in the failing heart. *Circulation* 2010;121:1912–25.
- [51] Kim YM, Pae HO, Park JE, Lee YC, Woo JM, Kim NH, et al. Heme oxygenase in the regulation of vascular biology: from molecular mechanisms to therapeutic opportunities. *Antioxid Redox Signal* 2011;14:137–67.
- [52] Foo RS, Siow RC, Brown MJ, Bennett MR. Heme oxygenase-1 gene transfer inhibits angiotensin II-mediated rat cardiac myocyte apoptosis but not hypertrophy. *J Cell Physiol* 2006;209:1–7.
- [53] Fernandes RO, Bonetto JH, Baregazy B, de Castro AL, Puukila S, Forsyth H, et al. Modulation of apoptosis by sulforaphane is associated with PGC-1α stimulation and decreased oxidative stress in cardiac myoblasts. *Mol Cell Biochem* 2015;401:61–70.
- [54] Lu Z, Xu X, Hu X, Fassett J, Zhu G, Tao Y, et al. PGC-1 α regulates expression of myocardial mitochondrial antioxidants and myocardial oxidative stress after chronic systolic overload. *Antioxid Redox Signal* 2010;13:1011–22.
- [55] Csala M, Kardon T, Legeza B, Lizák B, Mandl J, Margittai É, et al. On the role of 4-hydroxynonenal in health and disease. *Biochim Biophys Acta* 2015;1852:826–38.
- [56] Usatyuk PV, Parinandi NL, Natarajan V. Redox regulation of 4-hydroxy-2-nonenal-mediated endothelial barrier dysfunction by focal adhesion, adherens, and tight junction proteins. *J Biol Chem* 2006;281:35554–66.
- [57] Cohen G, Riahi Y, Sunda V, Deplano S, Chatgililoglu C, Ferreri C, et al. Signaling properties of 4-hydroxyalkenals formed by lipid peroxidation in diabetes. *Free Radic Biol Med* 2013;65:978–87.
- [58] Kang SM, Lim S, Song H, Chang W, Lee S, Bae SM, et al. Allopurinol modulates reactive oxygen species generation and Ca²⁺ overload in ischemia-reperfused heart and hypoxia-reoxygenated cardiomyocytes. *Eur J Pharmacol* 2006;535:212–9.
- [59] Kuwahara K, Saito Y, Kishimoto I, Miyamoto Y, Harada M, Ogawa E, et al. Cardiotrophin-1 phosphorylates Akt and BAD, and prolongs cell survival via a PI3K-dependent pathway in cardiac myocytes. *J Mol Cell Cardiol* 2000;32:1385–94.
- [60] Cai C, Teng L, Vu D, He JQ, Guo Y, Li Q, et al. The heme oxygenase 1 inducer (CoPP) protects human cardiac stem cells against apoptosis through activation of the extracellular signal-regulated kinase (ERK)/NRF2 signaling pathway and cytokine release. *J Biol Chem* 2012;287:33720–32.
- [61] Leoncini E, Malaguti M, Angeloni C, Motori E, Fabbri D, Hrelia S. Cruciferous vegetable phytochemical sulforaphane affects phase II enzyme expression and activity in rat cardiomyocytes through modulation of Akt signaling pathway. *J Food Sci* 2011;76:H175–81.
- [62] Ren J, Zhang S, Kovacs A, Wang Y, Muslin AJ. Role of p38α MAPK in cardiac apoptosis and remodeling after myocardial infarction. *J Mol Cell Cardiol* 2005;38:617–23.
- [63] Dhingra S, Sharma AK, Arora RC, Slezak J, Singal PK. IL-10 attenuates TNF-α-induced NF-κB pathway activation and cardiomyocyte apoptosis. *Cardiovasc Res* 2009;82:59–66.
- [64] Estañ MC, Calviño E, de Blas E, Boyano-Adán MC, Mena ML, Gómez-Gómez M, et al. 2-Deoxy-D-glucose cooperates with arsenic trioxide to induce apoptosis in leukemia cells: involvement of IGF-1R-regulated Akt/mTOR, MEK/ERK and LKB-1/AMPK signaling pathways. *Biochem Pharmacol* 2012;84:1604–16.
- [65] Nian M, Lee P, Khaper N, Liu P. Inflammatory cytokines and postmyocardial infarction remodeling. *Circ Res* 2004;94:1543–53.
- [66] Kwon JS, Joung H, Kim YS, Shim YS, Ahn Y, Jeong MH, et al. Sulforaphane inhibits restenosis by suppressing inflammation and the proliferation of vascular smooth muscle cells. *Atherosclerosis* 2012;225:41–9.